

Photocatalytic degradation of C.I. Acid Red 27 by immobilized ZnO on glass plates in continuous-mode

M.A. Behnajady^{a,*}, N. Modirshahla^a, N. Daneshvar^b, M. Rabbani^c

^a Research Laboratory, Department of Applied Chemistry, Islamic Azad University, Tabriz Branch, P.O. Box 1655, Tabriz, Islamic Republic of Iran

^b Water and Wastewater Treatment Research Laboratory, Department of Applied Chemistry, Faculty of Chemistry, University of Tabriz, C.P. 51664, Tabriz, Islamic Republic of Iran

^c Department of Applied Chemistry, Faculty of Chemistry, Islamic Azad University, North Tehran Branch, P.O. Box 19585/936, Tehran, Islamic Republic of Iran

Received 20 May 2006; received in revised form 25 July 2006; accepted 26 July 2006

Available online 31 July 2006

Abstract

The photocatalytic degradation of C.I. Acid Red 27 (AR27), an anionic monoazo dye of acid class, in aqueous solutions was investigated with immobilized ZnO catalyst on glass plates in a continuous-mode. In the slurry ZnO system the separation and recycling of the photocatalyst is practically difficult. Thus, ZnO was immobilized on solid supports to solve this problem. The removal percent increases with increasing the photoreactor volume and light intensity but it decreases when the flow rate is increased. With decreasing flow rate from 43 to 15 ml min⁻¹, the complete decolorization and degradation was obtained at around 748 and 1080 cm³ from photoreactor volume. The increase in the light intensity from 21.4 to 58.5 W m⁻² increases the decolorization from 23 to 57.6% and degradation from 17.5 to 37.8% for 374 cm³ of photoreactor volume. NH₄⁺, NO₃⁻, NO₂⁻ and SO₄²⁻ ions were analyzed as mineralization products of nitrogen and sulfur heteroatoms. Results showed that final concentration of SO₄²⁻ ions and N-containing mineralization products were less than the finally expected stoichiometric values. The positive slope of production of NH₄⁺, NO₃⁻ and NO₂⁻ shows that these compounds are initial products resulting directly from the initial attack on the nitrogen-to-nitrogen double bond (–N=N–) of the azo dye.

© 2006 Elsevier B.V. All rights reserved.

Keywords: Advanced oxidation processes (AOPs); UV/ZnO; Heterogenous photocatalysis; Immobilized ZnO catalyst; Decolorization; Continuous-flow photoreactor; C.I. Acid Red 27

1. Introduction

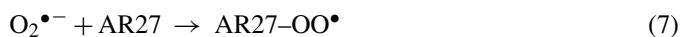
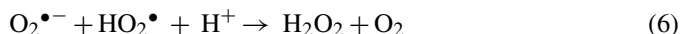
Dyes and pigments are used in many industries such as textile, leather, paper, pharmaceutical, paint, cosmetics, etc. Azo dyes constitute a major part of all commercial dyes [1]. Azo dyes and their derived products are known to present serious carcinogenic effect [2]. It is estimated that about 10% of the dye is lost during dyeing processes and released into wastewater [3]. The disposal of these colored wastewaters poses a major problem for the industry as well as a threat to the environment. The increased public concern about these compounds and the stringent international environmental standards (ISO 14001) have promoted the need to develop novel treatment methods for converting these organic dyes to harmless compounds [4]. C.I. Acid

Red 27 (AR27) was used as a food dye, textile dye for wool and silk as well as in photography [5]. However, in 1970, Russian studies [6] showed that AR27 was carcinogen.

Advanced oxidation processes (AOPs) are attractive alternatives to non-destructive physical water treatment processes, such as adsorption on activated carbon, flocculation and electrocoagulation, air stripping or desorption and membrane processes. The last techniques merely transport contaminants from one phase to another causing secondary pollution and requiring further treatment, whereas the former are able to mineralize aqueous organic contaminants [7]. From chemical, economical and ecotoxicological point of view, the ideal process must be able to destroy any organic pollutant to non-toxic and ubiquitous substances by its total oxidation. Under suitable operating conditions final products in AOPs are CO₂, H₂O and low molecular weight aliphatic acids [8]. Among the AOPs, combination of a semiconductor such as metal oxides (TiO₂, ZnO and Fe₂O₃) and metal sulfides (CdS and ZnS) as photocatalysts with UV light can be used for

* Corresponding author. Tel.: +98 411 3320198; fax: +98 411 3313922.
E-mail address: behnajady@iaut.ac.ir (M.A. Behnajady).

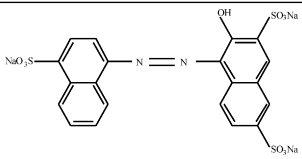
degradation of a wide range of organic contaminants [8–10]. The biggest advantage of ZnO in comparison with TiO₂ is that, it absorbs over a larger fraction of UV spectrum and the corresponding threshold of ZnO is 425 nm [10]. The prototype of a heterogenous photocatalytic reaction is based on the irradiation of particles of the semiconductor (ZnO) in the presence of dissolved molecular oxygen. The generally accepted mechanism of heterogenous photocatalysis includes redox reactions of adsorbed water, hydroxyl anions and oxygen molecules or other substances [11]. Upon irradiation, valence band electrons (e⁻) are promoted to the conduction band leaving a hole (h⁺) behind (Eq. (1)). These electron–hole pairs can either recombine (Eq. (2)) or interact separately with other molecules. The holes at the ZnO valence band can oxidize adsorbed water or hydroxide ions to produce hydroxyl radicals (Eqs. (3) and (4)). Electron in the conduction band on the catalyst surface can reduce molecular oxygen to superoxide anion (O₂^{•-}) (Eq. (5)). This radical may form organic peroxides (AR27–OO[•]) or hydrogen peroxide in the presence of organic scavengers (Eqs. (6) and (7)). The hydroxyl radical is a powerful oxidizing agent and attacks to organic compounds and intermediates (Int.) are formed. These intermediates react with hydroxyl radicals to produce final products (P) (Eq. (8)) [9–11]:



Since photocatalysts are often applied as suspension [8–10], hence, the separation of photocatalyst particles from its aqueous suspensions represents a serious problem for practical engineering [12]. Therefore, a key technique for simple applications seems to be the preparation of immobilized photocatalyst coatings on different substances without loss of photocatalytic activity [13,14]. Unfortunately little attention has been diverted to design continuous-flow photoreactors with immobilized photocatalyst on a solid surface [15–17]. Many techniques have been used for deposition of ZnO such as thermal physical vapor deposition [18], pulsed laser deposition [19], sputtering [20] and thermal oxidation [21].

In the present work we have described the construction and performance of a continuous-flow photoreactor with immobilized ZnO catalyst by heat attachment method on glass plates for decolorization and mineralization of AR27 as a model compound from anionic monoazo dye of acid class.

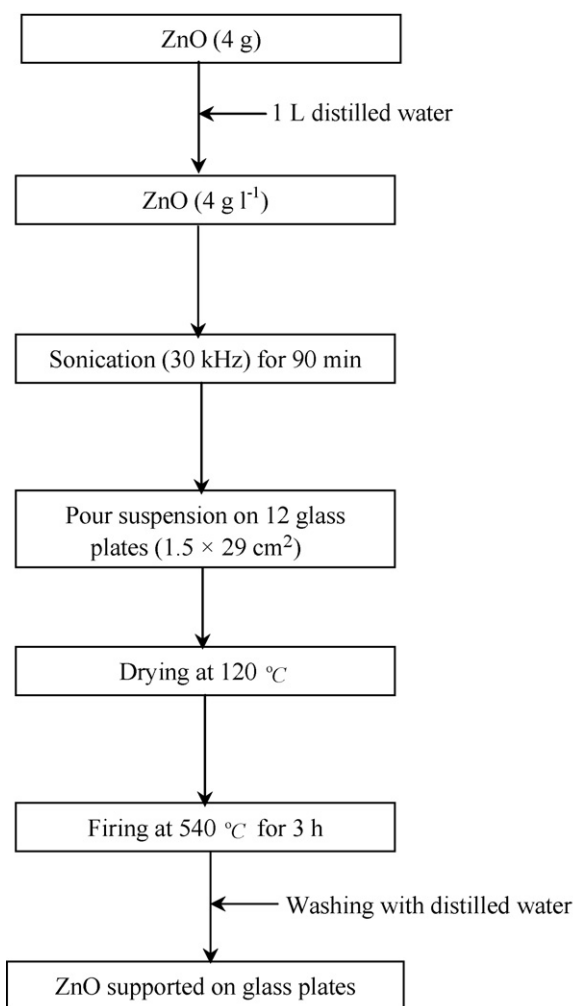
Table 1
Structure and characteristics of C.I. Acid Red 27 (AR27)

Structure	
Other names	Amaranth, Azorubin S, FD&C Red 2, Food Red 9
C.I. number	16185
λ _{max} (nm)	521
M _w (g mol ⁻¹)	604.48

2. Experimental

2.1. Materials

AR27, a monoazo anionic dye, was obtained from Boyakh Saz Company (Iran). Its chemical structure and other characteristics are listed in Table 1. ZnO was purchased from Merck (Germany).



Scheme 1. Schematic diagram of the heat attachment method for immobilization of ZnO on glass plates.

2.2. Immobilization of ZnO on glass plates

To prepare the immobilized ZnO on glass plates (1.5 cm × 29 cm) heat attachment method was used [13]. In this procedure, a suspension containing 4 g l⁻¹ ZnO in distilled water was prepared. Prepared suspension was sonicated in an ultrasonic bath (T460H, Windaus) under 30 kHz frequency for 90 min in order to improve the dispersion of ZnO in water. Glass plates treated with a dilute HF solution and washed in a solution of NaOH (0.01 M) in order to increase the number of OH groups and better contact of ZnO on glass plates. In this stage, sonicated suspension was poured on 12 glass plates and then placed in an oven at 120 °C. After drying, the glass plates were fired at 540 °C for 3 h. The glass plates were washed with distilled water for removing loosely attached ZnO particles (Scheme 1). The adhesion measurement and the amount of released ZnO can be detected from ZnO absorption band in UV range (387 nm) [12]. Double distilled water was pumped to photoreactor at the same conditions as decolorization experiments and the absorbance of the effluent water was measured at 378 nm to determine whether any ZnO was present. The results showed that ZnO particles had been attached strongly to glass plate surface. Fig. 1 shows scanning electron microscope (SEM) image of ZnO immobilized on glass plates. The loading of immobilized photocatalyst was measured to be 3.88 mg cm⁻².

2.3. Photoreactor

All experiments were carried out in a tubular continuous-flow photoreactor. Schematic diagram which has been shown in Fig. 2. The photoreactor comprises four quartz tubes (24.4 mm i.d., 26 mm o.d.), which were serially connected by means of transparent rubber tubes from the top to the bottom. The length of the photoreactor was 300 cm. Three ZnO loaded glass plates were inserted in each of quartz tubes. The radiation sources were four low pressure mercury UV lamps (30 W, UV-C, λ_{max} = 254 nm, 26 mm o.d., length = 90 cm, manufactured by Philips, Holland), which were placed in front of the quartz tubes.

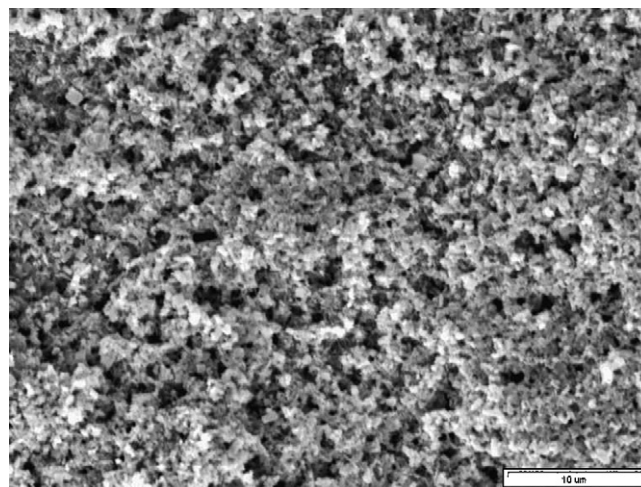


Fig. 1. SEM micrograph of immobilized ZnO on glass plate.

The variation of distance between the lamps and the quartz tubes caused the change of the light intensity.

2.4. Procedures

For photocatalytic degradation of AR27, a solution containing known concentration of AR27 was prepared and then 2 l of the prepared solution was transferred into a Pyrex beaker and agitated with a magnetic stirrer during experiment. For saturation of solution with oxygen, it was continuously purged with O₂ through a gas disperser placed at the bottom of the Pyrex beaker before and during the illumination. The solution was pumped with a peristaltic pump through the irradiated quartz tubes, and AR27 concentration at the inlet and outlet was analyzed with a UV-vis spectrophotometer (Ultrospec 2000, Biotech Pharmacia, England) at 521 and 254 nm. The absorbance at 521 nm is due to the color of the dye solution and it is used to monitor the decolorization of the dye. The absorbance at 254 nm represents the aromatic content of AR27 and absorbance decrease at 254 nm indicates the degradation of aromatic part of the dye [22].

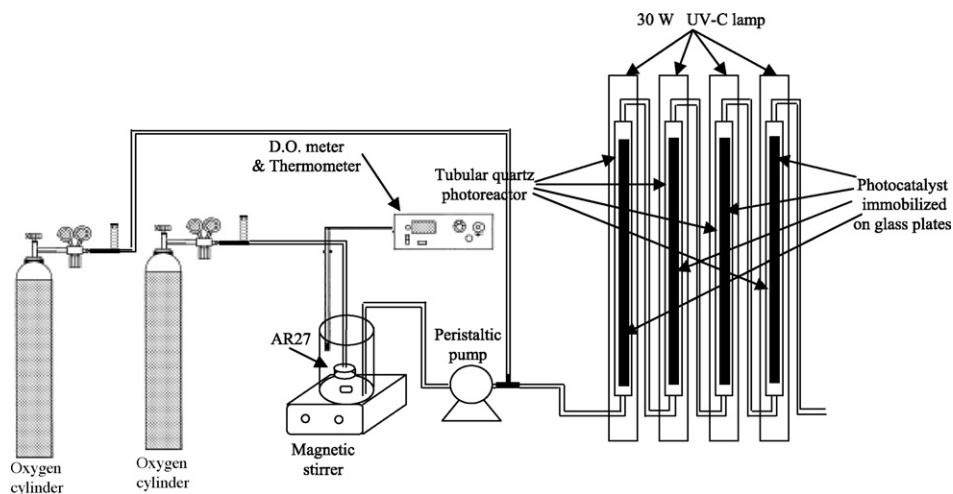


Fig. 2. Schematic diagram of tubular continuous-flow photoreactor. For details refer to text.

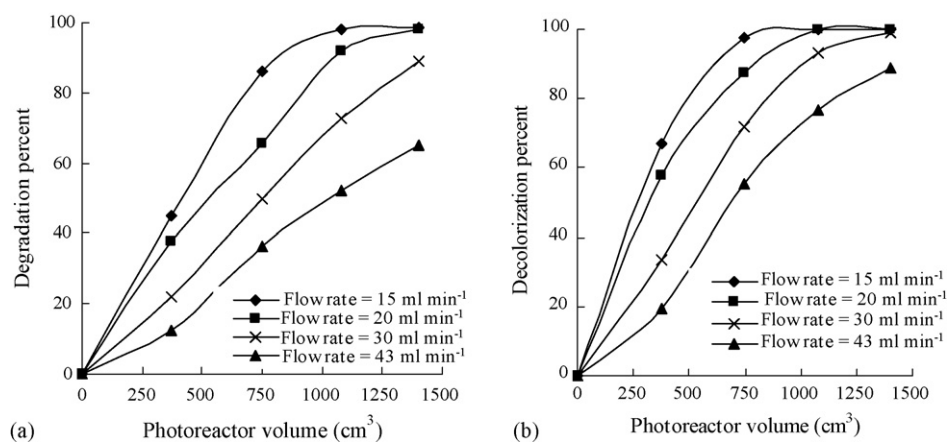


Fig. 3. Effect of the flow rate at degradation (a) and decolorization (b) of AR27 in UV/ZnO process at continuous-mode. $[AR27]_0 = 30 \text{ mg l}^{-1}$ and $I_0 = 58 \text{ W m}^{-2}$.

The degree of mineralization of AR27 in this system was monitored through UV–vis and COD analyses. The changes in the absorption spectra of AR27 at different volumes of photoreactor were recorded on a double-beam UV–vis spectrophotometer (Shimadzu 1700) in the wavelength range from 190 to 700 nm.

The formation of SO_4^{2-} , NH_4^+ and N in the forms of NO_3^- and NO_2^- ions were determined by turbidimetric, direct nesslerization and spectrophotometric methods, respectively [23]. Chemical oxygen demand (COD) was measured by the dichromate reflux method [24].

The light intensity in the center of the photoreactor was measured by a Lux-UV-IR meter (Leybold Co., GmbH). The SEM image of ZnO immobilized on glass plates was recorded with SEM Cambridge S360.

3. Results and discussion

3.1. Effect of the flow rate

The degradation and decolorization efficiency versus photoreactor volume at different flow rates have been summarized in Fig. 3a and b, respectively. The results indicate that with decreasing flow rate from 43 to 15 ml min^{-1} , removal efficiency increases, so that the complete decolorization and degradation were obtained at around 748 and 1080 cm^3 of photoreactor volume, respectively. This result is logical, because with decreasing flow rate the residence time of the reactant increases in the reactor.

3.2. Effect of the light intensity

The effect of the light intensity on the decolorization and degradation of AR27 was shown in Fig. 4. The results show that the removal percent steadily increased with increasing the light intensity linearly. The increase in the light intensity from 21.4 to 58.5 W m^{-2} increases the decolorization from 23 to 57.6% and degradation from 17.5 to 37.8% for 374 cm^3 of photoreactor volume. Previous studies indicated that at low light intensities, the reaction rate would increase linearly with increasing light intensity (first order), at intermediate light intensities the reaction

rate would depend on the square root of the light intensity (half order), and at high light intensities the reaction rate was independent of the light intensity [25]. The transition points between these regimes will vary with pollutant and photocatalyst species. The linear relation indicates that saturation of the catalyst by the incident photons was not reached and electron–hole pairs are consumed more rapidly by chemical reactions than by recombination, therefore the rate of formation of the electron–hole pairs is directly proportional to the light intensity [9]. This result reveals that the UV light intensities tested in this study lie within the linear range.

3.3. Mineralization and final products of degradation of AR27

Mineralization of AR27 in this process was studied by COD loss, changes in UV–vis spectra and also SO_4^{2-} , NH_4^+ , NO_3^- and NO_2^- evolution at different volumes of photoreactor.

3.3.1. Extent of COD removal

The changes in UV absorbance cannot reflect the extent of degradation and mineralization of AR27. COD values have been related to the total concentration of organics in the solution

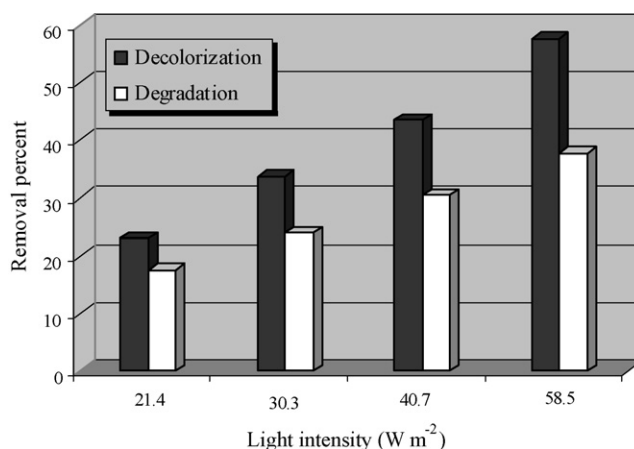


Fig. 4. Effect of the light intensity on degradation and decolorization of AR27. $[AR27]_0 = 30 \text{ mg l}^{-1}$ and residence time = 19 min.

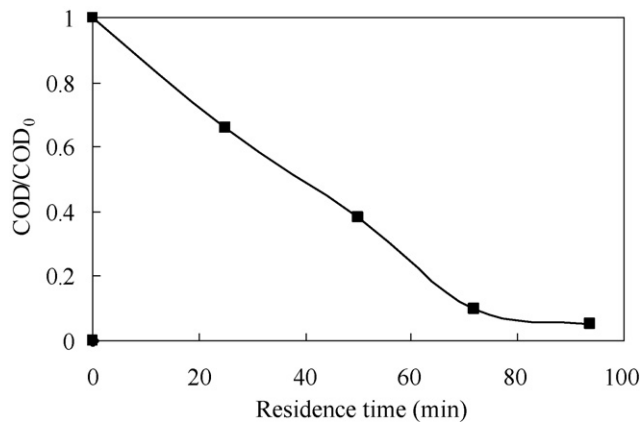


Fig. 5. COD changes vs. residence time. $[\text{AR27}]_0 = 30 \text{ mg l}^{-1}$ and $I_0 = 58 \text{ W m}^{-2}$.

and the decrease of COD reflects the degree of mineralization as a function of residence time. The result of COD removal as a function of residence time is shown in Fig. 5. It is worth mentioning that 90% mineralization could be achieved in 72 min residence time which shows immobilized ZnO on the surface of glass plates is photocatalytically active and suitable for mineralization of an organic dye such as AR27 in a continuous-mode.

3.3.2. Evaluation of final mineralization products

The formation of SO_4^{2-} ions versus residence time is presented in Fig. 6. According to the AR27 molecular structure in Table 1, the three sulfonic groups attached to two kinds of naphthalene rings. Fig. 6 shows the initial amount of SO_4^{2-} ions is very low for 25 min residence time. This result indicates that SO_4^{2-} ions are formed after decolorization stage and breakdown of nitrogen-to-nitrogen double bond ($-\text{N}=\text{N}-$) of the azo dye. The concentration of SO_4^{2-} ions in outlet stream from photoreactor was less than the expected value for complete min-

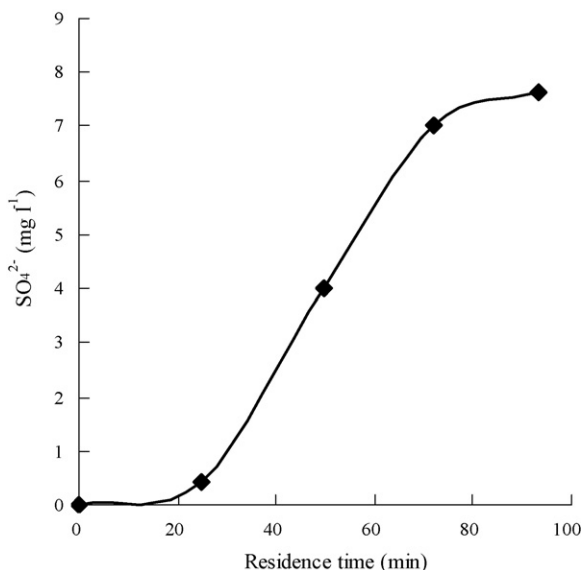


Fig. 6. SO_4^{2-} formation vs. residence time. $[\text{AR27}]_0 = 30 \text{ mg l}^{-1}$ and $I_0 = 58 \text{ W m}^{-2}$.

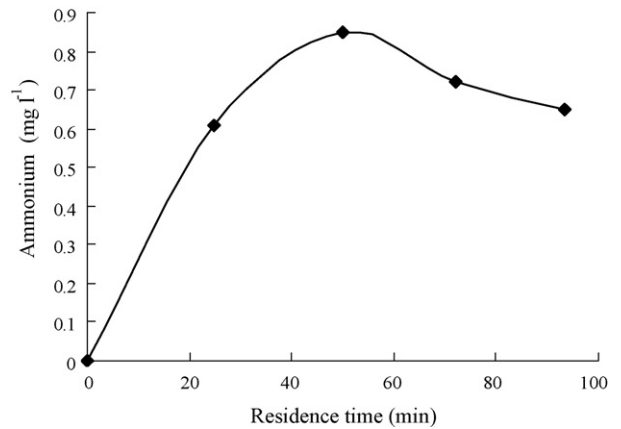


Fig. 7. NH_4^+ formation vs. residence time. For details refer to Fig. 6.

eralization of dye. This result can be concluded for the following reasons:

- a little amount of SO_4^{2-} ions is adsorbed on the photocatalyst surface [26];
- formation of sulfur dioxide [26,27];
- a little amount of S heteroatom can be attached to intermediate- SO_3^- .

The formation of NH_4^+ , NO_3^- and NO_2^- as N-containing mineralization products versus residence time are given in Figs. 7 and 8, respectively. The nitrogen mass balance, obtained with considering NH_4^+ , NO_3^- and NO_2^- concentrations, shows that the concentration of N-containing mineralization products is less than the final expected stoichiometric value. This could be explained by the formation of N_2 [28]. Figs. 7 and 8 show the initial slope is positive for NH_4^+ , NO_3^- and NO_2^- , indicating these ions are initial products, resulting directly from the initial attack on the nitrogen-to-nitrogen double bond ($-\text{N}=\text{N}-$) of the azo dye.

3.3.3. UV-vis absorption spectra

The changes in the UV-vis absorption spectra of AR27 solutions during the photocatalytic degradation run at differ-

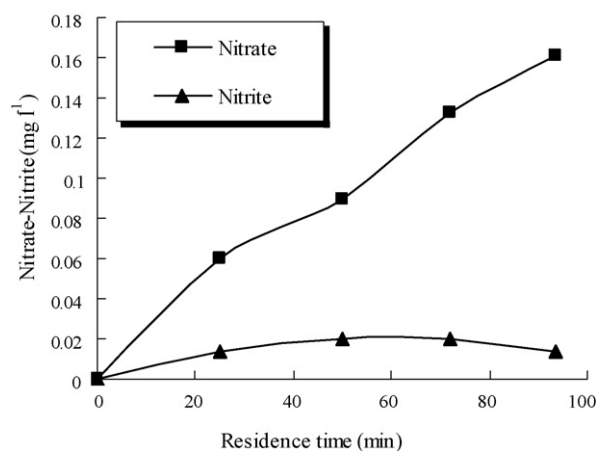


Fig. 8. NO_3^- and NO_2^- formation vs. residence time. For details refer to Fig. 6.

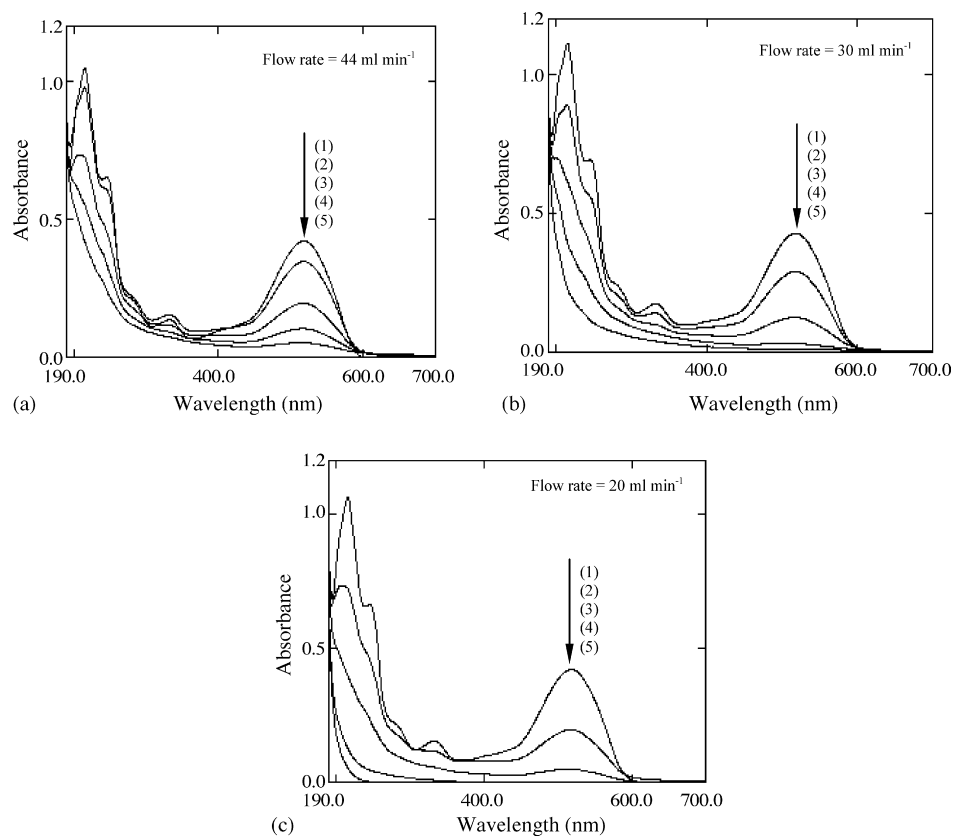


Fig. 9. UV–vis spectral changes of AR27, recorded during the dye degradation at different photoreactor volumes. (1) 0, (2) 374, (3) 748, (4) 1080 and (5) 1403 cm³. [AR27]₀ = 30 mg l⁻¹ and I₀ = 58 W m⁻².

ent photoreactor volumes and volumetric flow rates have been shown in Fig. 9. The decrease of the absorption peak of AR27 at $\lambda = 521$ nm in Fig. 9 indicated a rapid degradation of the azo dye. The decrease is also meaningful with respect to the nitrogen-to-nitrogen double bond ($-N=N-$) of the azo dye, as the most active site for oxidative attack. As can be seen from Fig. 9a, in the final outlet stream of photoreactor, absorption spectra in the UV–vis regions did not disappear for flow rate of 44 ml min⁻¹. With decreasing the flow rate to 20 ml min⁻¹, absorption spectrum in the UV–vis regions for final outlet stream of the photoreactor is reduced considerably (Fig. 9c).

4. Conclusions

UV/ZnO process with immobilized photocatalyst on glass plates in continuous-mode can be used for complete degradation of AR27 as a model compound from monoazo anionic dyes. Removal efficiency of AR27 in this process was very sensitive to photoreactor volume, volumetric flow rate and light intensity. The formation of NH₄⁺, NO₃⁻ and NO₂⁻ ions at the beginning of the reaction and rapid decrease of absorption peaks of AR27 at $\lambda = 521$ nm show that these ions were initial products resulting directly from the initial attack to the nitrogen-to-nitrogen double bond ($-N=N-$) of the azo dye. The formation of SO₄²⁻ ions at the beginning of the reaction was very low, which indicates that SO₄²⁻ ions were formed after decolorization stage.

Acknowledgement

The authors thank the Islamic Azad University of Tabriz branch for financial and other supports.

References

- [1] Kirk-Othmer, Encyclopedia of Chemical Technology, 3rd ed., John Wiley & Sons, 1978, pp. 387–433.
- [2] K. Golka, S. Kopps, Z.W. Myslak, Toxicol. Lett. 151 (2004) 203.
- [3] L. Young, J. Yu, Water Res. 31 (1997) 1187.
- [4] M. Styliidi, D.I. Kondarides, X.E. Verykios, Appl. Catal. B 40 (2003) 271.
- [5] M. Karkmaz, E. Puzenat, C. Guillard, J.M. Herrmann, Appl. Catal. B 51 (2004) 183–194.
- [6] M. Perez-Urquiza, J.L. Beltran, J. Chromatogr. A 898 (2000) 271.
- [7] M.A. Behnajady, N. Modirshahla, M. Shokri, Chemosphere 55 (2004) 129.
- [8] N. Daneshvar, D. Salari, M.A. Behnajady, Iran. J. Chem. Chem. Eng. 21 (2002) 55–62.
- [9] N. Daneshvar, M. Rabbani, N. Modirshahla, M.A. Behnajady, J. Photochem. Photobiol. A 168 (2004) 39–45.
- [10] M.A. Behnajady, N. Modirshahla, R. Hamzavi, J. Hazard. Mater. B 133 (2006) 226–232.
- [11] M.R. Hoffmann, S.T. Martin, W. Choi, D.W. Bahnemann, Chem. Rev. 95 (1995) 69.
- [12] J.A. Byrne, B.R. Eggins, N.M.D. Brown, B. McKinney, M. Rouse, Appl. Catal. B 17 (1998) 25–36.
- [13] M.R. Dhananjeyan, J. Kiwi, K.R. Thampi, Chem. Commun. (2000) 1443–1444.
- [14] S. Sakthivel, M.V. Shankar, M. Palanichamy, B. Arabinidoo, V. Murugesan, J. Photochem. Photobiol. A 148 (2002) 153–159.

- [15] M. Trillas, J. Peral, X. Domenech, *J. Chem. Technol. Biotechnol.* 67 (1996) 237–242.
- [16] K. Kobayakawa, C. Sato, Y. Sato, A. Fujishima, *J. Photochem. Photobiol. A* 118 (1998) 65–69.
- [17] G.R.R.A. Kumara, F.M. Sultanbawa, V.P.S. Perera, I.R.M. Kottegoda, K. Tennakone, *Solar Energy Mater. Solar Cells* 58 (1999) 167–171.
- [18] O.A. Fouad, A.A. Ismail, Z.I. Zaki, R.M. Mohamed, *Appl. Catal. B* 62 (2006) 144–149.
- [19] S. Choopun, H. Tabata, T. Kawai, *J. Cryst. Growth* 274 (2005) 167–172.
- [20] S.-S. Lin, J.-L. Huang, *Surf. Coat. Technol.* 185 (2004) 222–227.
- [21] Ya.I. Alivov, A.V. Chernykh, M.V. Chukichev, R.Y. Korotkov, *Thin Solid Films* 473 (2005) 241–246.
- [22] M. Muruganandham, M. Swaminathan, *Dyes Pigments* 62 (2004) 271–277.
- [23] ASTM, *Annual Book of ASTM Standards, Water and Environmental Technology*, vol. 11.01, ASTM, Philadelphia, PA, 2000.
- [24] APHA/AWWA/WPCF, *Standards Methods for the Examination of Water and Wastewater*, 17th ed., American Public Health Association, Washington, DC, 1989.
- [25] R. Terzian, N. Serpone, *J. Photochem. Photobiol. A* 89 (1995) 163–175.
- [26] E. Vulliet, C. Emmelin, J.M. Chovelon, C. Guillard, J.M. Herrmann, *Environ. Chem. Lett.* 1 (2003) 62–67.
- [27] V. Brezova, M. Jankovicova, M. Soldan, A. Blazkova, M. Rehakova, I. Surina, M. Ceppan, B. Havlinova, *J. Photochem. Photobiol. A* 83 (1994) 69–75.
- [28] H. Lachheb, E. Puzenat, A. Houas, M. Ksibi, E. Elaloui, C. Guillard, J.M. Herrmann, *Appl. Catal. B* 39 (2002) 75–90.